Modeling the Oxygen-Evolving Complex of Photosystem II. Synthesis, Redox Properties, and Core Interconversion Studies of Dimanganese Complexes Having $\{Mn^{III}_2(\mu\text{-}O)(\mu\text{-}OAc)_2\}^{2+}$, $\{Mn^{III}Mn^{IV}(\mu\text{-}O)_2(\mu\text{-}OAc)\}^{2+}$, and $\{Mn^{IV}_2(\mu\text{-}O)_2(\mu\text{-}OAc)\}^{3+}$ Cores with MeL as a Terminal Ligand: A New Asymmetric Mixed-Valence Core[†,1]

Tapan Kumar Lal and Rabindranath Mukherjee*

Department of Chemistry, Indian Institute of Technology, Kanpur 208 016, India

Received December 3, 1997

The synthesis of $[Mn^{III}Mn^{IV}(\mu\text{-}O)_2(\mu\text{-}OAc)(MeL)_2][ClO_4]_2\cdot H_2O$ (**1a**), $[Mn^{III}Mn^{IV}(\mu\text{-}O)_2(\mu\text{-}OAc)(MeL)_2][BF_4]_2\cdot$-2MeCN (**1b**), $[Mn^{III}_2(\mu\text{-}O)(\mu\text{-}OAc)_2(MeL)_2][PF_6]_2\cdot H_2O$ (**2a**), $[Mn^{III}_2(\mu\text{-}O)(\mu\text{-}OAc)_2(MeL)_2][ClO_4]_2\cdot H_2O$ (**2b**), and $[Mn^{IV}_2(\mu\text{-}O)_2(\mu\text{-}OAc)(MeL)_2][ClO_4]_3\cdot H_2O$ (**3**), containing a common tridentate facially capping ligand with chelate ring asymmetry, (2-pyridylmethyl)(2-pyridylethyl)methylamine (MeL), is described. X-ray crystallographic analysis of complex **1b** revealed that it has an asymmetric $Mn^{III}Mn^{IV}(\mu\text{-}O)_2(\mu\text{-}OAc)\}^{2+}$ core, as a result of different binding modes adopted by MeL at the Mn(III) versus the Mn(IV) site. The present group of complexes have both kinds of dimanganese core structure as that in the proposed tetranuclear structural model for the OEC in PSII. Temperature-dependent magnetic properties reveal the following results: $2J = -288$, -244, and $+2$ cm^{-1} for **1a**, **3**, and **2a**, respectively. Complex **1a** has a doublet ground state and its X-band EPR spectrum at 77 K exhibits a 16-line pattern at $g = 2$. Owing to their substitutional lability, various core interconversion studies have been done on **1a**, **2b**, and **3**, in considerable detail. The redox properties of **1a**, **2a**, and **3** have been systematically investigated. Complex **1a** is reversibly oxidized by a one-electron process at 1.0 V to generate the Mn^{IV}_2 dimer and is reduced irreversibly to Mn^{III}_2 species at -0.1 V vs SCE. Complex **3** exhibits two reductive redox processes at potentials almost identical (within experimental error) to that of **1a**. Complex **2a** displays a scan-rate dependent oxidative process at 1.2 V; an irreversible reductive process is also observed to generate $Mn^{III}Mn^{II}$ species at 0.0 V vs SCE. On cycling of the scans between the potential limits 0.4 to 1.4 V, at the expense of the higher potential response at 1.0 V the lower potential response at 0.82 V grows. Coulometric oxidation of **2a** at 1.2 V reveals that a net two-electron has been released, thereby generating one-electron oxidized form of **1a**, due to an ECE mechanism. The successes of the synthetic reactions and the core interconversion studies presented here are the consequences of a series of disproportionation reactions. For **2a** the electron-transfer processes are accompanied by protonation/deprotonation phenomena of relevance to OEC in PSII. To pinpoint the role of Cl^- during redox transitions in OEC, the reactions of chloride ion with **1a**, **2b**, and **3** have been investigated by means of absorption spectroscopy and cyclic voltammetry.

Introduction

Oxo-bridged bi-, tri-, and tetranuclear manganese complexes are of considerable current interest as they serve as good synthetic models for the active site of the OEC of PSII.[2−5] Proposed mechanisms for water oxidation involve sequential redox steps of the Mn centers (II, III, and IV oxidation levels) accompanied by protonation/deprotonation at the bridging oxo groups.[2b,5] This interplay of protonation/deprotonation with redox reactions of the Mn center is important in controlling the kinetic and thermodynamic stability of the Mn cluster.

Recently, a tetranuclear structural model for the OEC in PSII has been proposed[6] involving two bis(μ-oxo)dimanganese units linked by μ-oxo bis(μ-carboxylato) bridges. Hence studies aimed at systematic investigation of the redox properties and core interconversion studies of "first generation models"[7] having the above-mentioned binuclear structural motifs with manganese in various oxidation levels are highly desirable to gain more insight into the functional aspects of OEC in PSII.

Synthetic model studies have led to the discovery of a variety of interesting binuclear structural units $\{Mn_2(\mu\text{-}O)(\mu\text{-}O_2CR)\}$,[8]

[†] Dedicated to Professor Animesh Chakravorty on the occasion of his 63rd birthday.

(1) Abbreviations used: MeL, (2-pyridylethyl)(2-pyridylmethyl)methylamine; bpea, *N*,*N*-bis(2-pyridylmethyl)ethylamine; tacn, 1,4,7-triazacyclononane; Me_3tacn, *N*,*N*′,*N*″-trimethyl-1,4,7-triazacyclononane; OAc^-, acetate ion; OEC, oxygen-evolving complex; PSII, photosystem II; IR, infrared; EPR, electron paramagnetic resonance; CV, cyclic voltammetry; SCE, saturated calomel electrode.

(2) (a) Rüttinger, W.; Dismukes, G. C. *Chem. Rev.* **1997**, *97*, 1. (b) Manchanda, R.; Brudvig, G. W.; Crabtree, R. H. *Coord. Chem. Rev.* **1995**, *144*, 1 and references therein. (c) Brudvig, G. W.; Thorp, H. H.; Crabtree, R. H. *Acc. Chem. Res.* **1991**, *24*, 311. (d) Thorp, H. H.; Brudvig, G. W. *New J. Chem.* **1991**, *15*, 479.

(3) (a) Pecoraro, V. L.; Baldwin, M. J.; Gelasco, A. *Chem. Rev.* **1994**, *94*, 807. (b) Dismukes, G. C. *Bioinorganic Catalysis*; Reedijk, J., Ed.; Marcell Dekker Inc.: New York, 1992; Chapter 10, p 317.

(4) (a) Que, L., Jr.; True, A. E. *Prog. Inorg. Chem.* **1989**, *37*, 99. (b) Vincent, J. B.; Christou, G. *Advances in Inorganic Chemistry*; Sykes, A. G., Ed.; Academic Press: New York, San Diego, **1989**; Vol. 33, p 197. (c) Brudvig, G. W.; Crabtree, R. H. *Prog. Inorg. Chem.* **1989**, *37*, 99. (d) Wieghardt, K. *Angew. Chem., Int. Ed. Engl.* **1989**, *28*, 1153. (e) Renger, G. *Angew. Chem., Int. Ed. Engl.* **1987**, *26*, 643.

(5) (a) Baldwin, M. J.; Pecoraro, V. L. *J. Am. Chem. Soc.* **1996**, *118*, 11325. (b) Carroll, J. M.; Norton, J. R. *J. Am. Chem. Soc.* **1992**, *114*, 8744.

(6) (a) Yachandra, V. K.; DeRose, V. J.; Latimer, M. J.; Mukerji, I.; Sauer, K.; Klein, M. P. *Science* **1993**, *260*, 675. (b) Wieghardt, K. *Angew. Chem., Int. Ed. Engl.* **1994**, *33*, 725.

S0020-1669(97)01514-0 CCC: $15.00
Published on Web 05/02/1998

$\{Mn_2(\mu\text{-}O)(\mu\text{-}O_2CR)_2\}$,[7a,9−11a] $\{Mn_2(\mu\text{-}O)_2(\mu\text{-}O_2CR)\}$,[9e,f,11b,12−14] and $\{Mn_2(\mu\text{-}O)_2\}$[7b,c,15−19] with manganese in (III,IV), (III,III), and (IV,IV) oxidation levels. In these complexes terminal coordination sites are provided primarily by a variety of neutral N-donor ligands. Investigations on these molecules have enriched our knowledge with new structural types and our understanding of detailed electronic structures[20] of these cores. It is worth mentioning here that to date no single system has been obtained in which all three forms $Mn^{III}Mn^{IV}$, $Mn^{III}{}_2$, and $Mn^{IV}{}_2$ with oxo-/acetato-bridging have been isolated using a common facially capping tridentate N-donor ligand.[21] Although the bpy systems[10b−e,14] for which binuclear complexes having all three forms have been isolated, they have not been reported to exhibit reversible electrochemistry giving an opportunity to systematically investigate the redox properties of both $\{Mn_2O(O_2CR)_2\}$ and $\{Mn_2O_2(O_2CR)\}$ cores with a given terminal ligand, for a better description of the structures and possible core interconversion studies between the various oxidation levels of manganese. Noteworthy electrochemical investigations associated with protonation/deprotonation at the oxo bridge are only with the $\{Mn_2O_2\}$ core structure.[2b,22] Such studies directed toward $\{Mn^{III}{}_2O(OAc)_2\}$ to $\{Mn^{III}Mn^{IV}O_2(OAc)\}$ core interconversion have received only sporadic attention and that too not in an extensive manner.[9e,23] An interesting phenomenon which has attracted a comparatively limited number of systematic investigations[10c,12a,e,14a] using binuclear Mn centers[24] is the role of chloride ion, required for efficient water oxidation by OEC in PSII.[4e]

As a part of our work in exploring oxo-bridged binuclear Mn complexes supported by acetate bridges[11] with use of the tridentate facially capping ligand with chelate ring asymmetry (MeL),[26] we have now accomplished the synthesis of a $Mn^{IV}{}_2$ complex. We report here the full description of a comprehen-

(7) (a) Tanase, T.; Lippard, S. J. *Inorg. Chem.* **1995**, *34*, 4682. (b) Chan, M. K.; Armstrong, W. H. *J. Am. Chem. Soc.* **1991**, *113*, 5055. (c) Suzuki, M.; Hayashi, Y.; Munezawa, K.; Suenaga, M.; Senda, H.; Uehara, A. *Chem. Lett.* **1991**, 1929.

(8) Terminal tetradentate ligand coordination: (a) Arulsamy, N.; Glerup, J.; Hazell, A.; Hodgson, D. J.; McKenzie, C. J.; Toftlund, H. *Inorg. Chem.* **1994**, *33*, 3023. (b) Oberhausen, K. J.; O'Brien, R. J.; Richardson, J. F.; Buchanan, R. M.; Costa, R.; Latour, J.-M.; Tsai, H.-L.; Hendrickson, D. N. *Inorg. Chem.* **1993**, *32*, 4561.

(9) Terminal tridentate ligand coordination: (a) Gultneh, Y.; Ahvaji, B.; Raja Khan, A.; Butcher, R. J.; Tuchagues, J. P. *Inorg. Chem.* **1995**, *34*, 3633. (b) Wu, F.-J.; Kurtz, D. M., Jr.; Hagen, K. S.; Nyman, P. D.; Debrunner, P. G.; Vankai, V. A. *Inorg. Chem.* **1990**, *29*, 5174. (c) Toftlund, H.; Markiewicz, A.; Murray, K. S. *Acta Chem. Scand.* **1990**, *44*, 443. (d) Bossek, U.; Wieghardt, K.; Nuber, B.; Weiss, J. *Inorg. Chim. Acta* **1989**, *165*, 123. (e) Wieghardt, K.; Bossek, U.; Nuber, B.; Weiss, J.; Bonvoisin, J.; Corbella, M.; Vitols, S. E.; Girerd, J.-J. *J. Am. Chem. Soc.* **1988**, *110*, 7398. (f) Sheats, J. E.; Czernuszewicz, R. S.; Dismukes, G. C.; Rheingold, A. L.; Petrouleas, V.; Stubbe, J.; Armstrong, W. H.; Beer, R. H.; Lippard, S. J. *J. Am. Chem. Soc.* **1987**, *109*, 1435. (g) Wieghardt, K.; Bossek, U.; Bonvoisin, J.; Beauvillain, P.; Girerd, J.-J.; Nuber, B.; Weiss, J.; Heinze, J. *Angew. Chem., Int. Ed. Engl.* **1986**, *25*, 1030. (h) Wieghardt, K.; Bossek, U.; Ventur, D.; Weiss, J. *J. Chem. Soc., Chem. Commun.* **1985**, 347.

(10) Terminal bidentate and monodentate coordination: (a) Corbella, M.; Costa, R.; Ribas, J.; Fries, P. H.; Latour, J.-M.; Öhrström, L.; Solans, X.; Rodríguez, V. *Inorg. Chem.* **1996**, *35*, 1857. (b) Reddy, K. R.; Rajasekharan; Sukumar, S. *Polyhedron* **1996**, *15*, 4161. (c) Vincent, J. B.; Tsai, H.-L.; Blackman, A. G.; Wang, S.; Boyd, P. D. W.; Folting, K.; Huffman, J. C.; Lobkovsky, E. B.; Hendrickson, D. N.; Christou, G. *J. Am. Chem. Soc.* **1993**, *115*, 12353. (d) Blackman, A. G.; Huffman, J. C.; Lobkovsky, E. B.; Christou, G. *J. Chem. Soc., Chem. Commun.* **1991**, 989. (e) Ménage, S.; Girerd, J.-J.; Gleizes, A. *J. Chem. Soc., Chem. Commun.* **1988**, 431.

(11) Terminal asymmetric tridentate ligand coordination: (a) Mahapatra, S.; Lal, T. K.; Mukherjee, R. N. *Inorg. Chem.* **1994**, *33*, 1579. (b) Mahapatra, S.; Das, P.; Mukherjee, R. N. *J. Chem. Soc., Dalton Trans.* **1993**, 215.

(12) Terminal tridentate ligand coordination: (a) Pal, S.; Olmstead, M. M.; Armstrong, W. H. *Inorg. Chem.* **1995**, *34*, 4708 and references therein. (b) Pal, S.; Armstrong, W. H. *Inorg. Chem.* **1992**, *31*, 5417. (c) Pal, S.; Chan, M. K.; Armstrong, W. H. *J. Am. Chem. Soc.* **1992**, *114*, 6398. (d) Pal, S.; Gohdes, J. W.; Wilisch, W. C. A.; Armstrong, W. H. *Inorg. Chem.* **1992**, *31*, 713. (e) Wieghardt, K.; Bossek, U.; Zsolnai, L.; Huttner, G.; Blondin, G.; Girerd, J.-J.; Babonneau, F. *J. Chem. Soc., Chem. Commun.* **1987**, 651.

(13) One terminal tridentate and the other bidentate/monodentate ligand coordination: Bossek, U.; Saher, M.; Weyhermüller, T.; Wieghardt, K. *J. Chem. Soc., Chem. Commun.* **1992**, 1780.

(14) Terminal bidentate and Cl^-/water ligand coordination: (a) Bashkin, J. S.; Schake, A. R.; Vincent, J. B.; Chang, H.-R.; Quioying, L.; Huffman, J. C. Christou, G.; Hendrickson, D. N. *J. Chem. Soc., Chem. Commun.* **1988**, 700. (b) Reddy, K. R.; Rajasekharan, M. V.; Padhye, S.; Dahan, F.; Tuchagues, J.-P. *Inorg. Chem.* **1994**, *33*, 428. (c) Dave, B. C.; Czernuszewicz, R. S.; Bond, M. R. Carrano, C. J. *Inorg. Chem.* **1993**, *32*, 3593.

(15) Terminal tetradentate ligand coordination: (a) Glerup, J.; Goodson, P. A.; Hazell, A.; Hazell, R.; Hodgson, D. J.; McKenzie, C. J.; Michelsen, K.; Rychlewska, U.; Toftlund, H. *Inorg. Chem.* **1994**, *33*, 4105. (b) Goodson, P. A.; Hodgson, D. J.; Glerup, J.; Michelsen, K.; Weihe, H. *Inorg. Chim. Acta* **1992**, *197*, 141. (c) Goodson, P. A.; Glerup, J.; Hodgson, D. J.; Michelsen, K.; Weihe, H. *Inorg. Chem.* **1991**, *30*, 4909. (d) Goodson, P. A.; Hodgson, D. J.; Michelsen, K. *Inorg. Chim. Acta* **1990**, *172*, 49. (e) Goodson, P. A.; Oki, A. R.; Glerup, J.; Hodgson, D. J. *J. Am. Chem. Soc.* **1990**, *112*, 6248. (f) Oki, A. R.; Glerup, J.; Hodgson, D. J. *Inorg. Chem.* **1990**, *29*, 2435. (g) Goodson, P. A.; Glerup, J.; Hodgson, D. J.; Michelsen, K.; Pedersen, E. *Inorg. Chem.* **1990**, *29*, 503. (h) Towle, D. K.; Botsford, C. A.; Hodgson, D. J. *Inorg. Chim. Acta* **1988**, *141*, 167.

(16) Terminal tetradentate ligand coordination: (a) Brewer, K. J.; Calvin, M.; Lumpkin, R. S.; Otvos, J. W.; Spreer, L. O. *Inorg. Chem.* **1989**, *28*, 4446. (b) Hagen, K. S.; Armstrong, W. H.; Hope, H. *Inorg. Chem.* **1988**, *27*, 967. (c) Suzuki, M.; Senda, H.; Kobayashi, Y.; Oshio, H.; Uehara, A. *Chem. Lett.* **1988**, 1763. (d) Suzuki, M.; Tokura, S.; Suhara, M.; Uehara, A. *Chem. Lett.* **1988**, 477.

(17) Terminal two bidentate ligand coordination: (a) Manchanda, R.; Brudvig, G. W.; Gala, S. de; Crabtree, R. H. *Inorg. Chem.* **1994**, *33*, 5157 and references therein. (b) Libby, E.; Webb, R. J.; Streib, W. E.; Folting, K.; Huffman, J. C.; Hendrickson, D. N.; Christou, G. *Inorg. Chem.* **1989**, *28*, 4743. (d) Cooper, S. R.; Dismukes, G. C.; Klein, M. P. *J. Am. Chem. Soc.* **1978**, *100*, 7248. (e) Cooper, S. R.; Calvin, M. *J. Am. Chem. Soc.* **1977**, *99*, 6623. (f) Plaksin, P. M.; Stoufer, R. C.; Mathew, M.; Palenik, G. J. *J. Am. Chem. Soc.* **1972**, *94*, 2121.

(18) Terminal tridentate ligand coordination: Kitajima, N.; Singh, U. P.; Amagai, H.; Osawa, M.; Moro-oka, Y. *J. Am. Chem. Soc.* **1991**, *113*, 7757.

(19) Terminal tetradentate ligand coordination: Larson, E.; Lah, M. S.; Li, X.; Bonadies, J. A.; Pecoraro, V. L. *Inorg. Chem.* **1992**, *31*, 373.

(20) (a) Gamelin, D. R.; Kirk, M. L.; Stemmler, T. L.; Pal, S.; Armstrong, W. H.; Penner-Hahn, J. E.; Solomon, E. I. *J. Am. Chem. Soc.* **1994**, *116*, 2392. (b) Kirk, M. L.; Chan, M. K.; Armstrong, W. H.; Solomon, E. I. *J. Am. Chem. Soc.* **1992**, *114*, 10432.

(21) (a) A peroxo-bridged binuclear complex having the $\{Mn^{IV}{}_2(\mu\text{-}O)_2(\mu\text{-}O_2)\}^{2+}$ core was reported by Wieghardt et al. with Me_3tacn as the terminal ligand: Bossek, U.; Weyhermüller, T.; Wieghardt, K.; Nuber, B.; Weiss, J. *J. Am. Chem. Soc.* **1990**, *112*, 6387. (b) Using the same terminal ligand, very recently they have reported a dimeric complex having the $\{Mn^{IV}{}_2(\mu\text{-}O)(\mu\text{-}PhBO_2)_2\}^{2+}$ core: Bossek, U.; Hummel, H.; Weyhermüller, T.; Wieghardt, K.; Russell, S.; van der Wolf, L.; Kolb, U. *Angew. Chem., Int. Ed. Engl.* **1996**, *35*, 1552.

(22) (a) Manchanda, R.; Thorp, H. H.; Brudvig, G. W.; Crabtree, R. H. *Inorg. Chem.* **1992**, *31*, 4040. (b) Manchanda, R.; Thorp, H. H.; Brudvig, G. W.; Crabtree, R. H. *Inorg. Chem.* **1991**, *30*, 494. (c) Thorp, H. H.; Sarneski, J. E.; Brudvig, G. W.; Crabtree, R. H. *J. Am. Chem. Soc.* **1989**, *111*, 9249.

(23) Manchanda, R.; Brudvig, G. W.; Crabtree, R. H.; Sarneski, J. E.; Didiuk, M. *Inorg. Chim. Acta* **1993**, *212*, 135.

(24) Chloride ion ligated Mn_4 complexes, however, have been thoroughly studied.[25]

(25) (a) Wemple, M. W.; Tsai, H.-L.; Folting, K.; Hendrickson, D. N.; Christou, G. *Inorg. Chem.* **1993**, *32*, 2025. (b) Hendrickson, D. N.; Christou, G.; Schmitt, E. A.; Libby, E.; Bashkin, J. S.; Wang, S.; Tsai, H.-L.; Vincent, J. B.; Boyd, P. D. W.; Huffman, J. C.; Folting, K.; Li, Q.; Streib, W. E. *J. Am. Chem. Soc.* **1992**, *114*, 2455. (c) Wang, S.; Tsai, H.-L.; Streib, W. E.; Christou, G.; Hendrickson, D. N. *J. Chem. Soc., Chem. Commun.* **1992**, 1427. (d) Wang, S.; Folting, K.; Streib, W. E.; Schmitt, E. A.; McCusker, J. K.; Hendrickson, D. N.; Christou, G. *Angew. Chem., Int. Ed. Engl.* **1991**, *30*, 305.

(26) (a) Mahapatra, S.; Gupta, N.; Mukherjee, R. N. *J. Chem. Soc., Dalton Trans.* **1992**, 3041. (b) Gupta, N.; Mukerjee, S.; Mahapatra, S.; Ray, M.; Mukherjee, R. N. *Inorg. Chem.* **1992**, *31*, 139.

sive synthetic methodology to isolate binuclear $Mn^{III}Mn^{IV}$, Mn^{III}_2, and Mn^{IV}_2 dimers. The dimers $[Mn^{III}Mn^{IV}(\mu\text{-}O)_2(\mu\text{-}OAc)(MeL)_2][ClO_4]_2\cdot H_2O$ (**1a**), $[Mn^{III}Mn^{IV}(\mu\text{-}O)_2(\mu\text{-}OAc)(MeL)_2][BF_4]_2\cdot 2MeCN$ (**1b**), $[Mn^{III}_2(\mu\text{-}O)(\mu\text{-}OAc)_2(MeL)_2][PF_6]_2\cdot H_2O$ (**2a**), $[Mn^{III}_2(\mu\text{-}O)(\mu\text{-}OAc)_2(MeL)_2][ClO_4]_2\cdot H_2O$ (**2b**), and $[Mn^{IV}_2(\mu\text{-}O)_2(\mu\text{-}OAc)(MeL)_2][ClO_4]_3\cdot H_2O$ (**3**) have been isolated, and complex **1b** has been structurally characterized to unravel a new asymmetric binuclear trapped valence core. A complete electrochemical analysis of these complexes, the core interconversion studies with $Mn^{III}Mn^{IV}$, Mn^{III}_2, and Mn^{IV}_2 oxidation levels, understanding the nature of various synthetic reactions, and reactivity studies of these cores toward chloride ion are the direct consequences of the successful syntheses of these complexes. It is understandable that the present studies would be of widespread chemical interest in augmenting our understanding of the structure−function relationships of OEC in various "*S*-states". Preliminary results for the complexes $[Mn^{III}Mn^{IV}(\mu\text{-}O)_2(\mu\text{-}OAc)(MeL)_2][ClO_4]_2\cdot H_2O$ (**1a**) and $[Mn^{III}_2(\mu\text{-}O)(\mu\text{-}OAc)_2(MeL)_2][PF_6]_2\cdot H_2O$ (**2a**) were briefly described previously.[11]

Experimental Section

Materials and Methods. Commercial reagents were used as obtained without further purification, unless stated otherwise. Acetonitrile (MeCN) was dried as before,[11] and methanol was dried over $Mg(OMe)_2$. Ethyl acetate was dried by distillation over anhydrous K_2CO_3.

Syntheses. (2-Pyridylethyl)(2-pyridylmethyl)methylamine. This was prepared as reported previously.[26b]

$[Mn^{III}Mn^{IV}(\mu\text{-}O)_2(\mu\text{-}OAc)(MeL)_2][ClO_4]_2\cdot H_2O$ (1a). Method A. This was synthesized using $Mn(OAc)_3\cdot 2H_2O$ as starting material under a dinitrogen atmosphere.[11b]

Method B. To a magnetically stirred solution of $Mn(OAc)_3\cdot 2H_2O$ (0.590 g, 2.202 mmol) and MeL (0.500 g; 2.202 mmol) in 12 mL of CH_3OH was added dropwise a solution of $HClO_4$ (0.3 mL of 70% $HClO_4$ dissolved in 3 mL of CH_3OH). The solution was stirred for 45 min during which time a green solid appeared. The solid was collected by filtration and washed thoroughly with CH_3OH. Recrystallization was achieved from CH_2Cl_2, and the product was dried in vacuo. Yield: 0.35 g, 37%. IR (KBr, cm^{-1}, selected peaks): 3430 (m, ν(OH)), 1565 (m, ν_{asym} (CO), 1440 (s, ν_{sym} (CO)), 1100 and 620 (s, $\nu(ClO_4^-)$, 720 (s, ν(MnOMn)). Absorption spectrum [in MeCN; λ_{max}, nm (ϵ, M^{-1} cm^{-1})]: 800 (sh) (150), 640 (350), 548 (300), 440 (sh) (750), 400 (sh) (1100), 259 (21 000). Conductivity (MeCN, 10^{-3} M solution at 298 K): Λ_M = 295 mho cm^2 mol^{-1}.

$[Mn^{III}Mn^{IV}(\mu\text{-}O)_2(\mu\text{-}OAc)(MeL)_2][BF_4]_2\cdot 2MeCN$ (1b). To a stirred mixture of $Mn(OAc)_3\cdot 2H_2O$ (0.1 g, 0.372 mmol), NaOAc (0.062 g, 0.746 mmol), and $NaBF_4$ (0.082 g, 0.746 mmol) in 5 mL of MeCN was added a solution of MeL (0.084 g, 0.372 mmol) in 5 mL of MeCN. The reaction mixture was stirred for 2 h. After filtration the volume of the filtrtate was reduced to ∼ 5 mL in vacuo. To it 5 mL of ethyl acetate was added, and the solution was kept at 273 K for 12 h. Green crystals thus formed were collected by filtration, washed thoroughly with ethyl acetate, and dried in vacuo. Yield: 0.06 g, 35%. Single crystals suitable for X-ray diffraction studies were grown by diffusion of ethyl acetate into a MeCN solution of the product.

$[Mn^{III}_2(\mu\text{-}O)(\mu\text{-}OAc)_2(MeL)_2][PF_6]_2\cdot H_2O$ (2a).[11a] To a stirred mixture of $Mn(OAc)_3\cdot 2H_2O$ (0.40 g, 1.5 mmol) and NH_4PF_6 (0.24 g, 1.49 mmol) in 10 mL of degassed MeCN, MeL (0.34 g, 1.49 mmol) dissolved in 10 mL of MeCN was added and the mixture stirred for 2 h at 298 K. It was then filtered, and solvent was reduced to ∼10 mL. To the purplish brown filtrate 3 mL of glacial acetic acid and 10 mL of ethyl acetate were added and allowed to stand for 24 h at 273 K. The purplish brown product thus obtained was collected by filtration and pumped to dryness in vacuo at 298 K. Yield: 0.90 g (60%). Anal. Calcd for $C_{32}H_{42}N_6O_6F_{12}P_2Mn_2$: C, 38.15; H, 4.17; N, 8.35. Found: C, 37.96; H, 4.10; N, 8.82. IR (KBr, cm^{-1}, selected peaks): 3420 (m, ν(OH)), 1575 (m, ν_{asym} (CO), 1435 (s, ν_{sym} (CO)), 835 (s, $\nu(PF_6^-)$, 760 (s, ν_{as} (MnOMn)). Absorption spectrum [in MeCN; λ_{max}, nm (ϵ, M^{-1} cm^{-1})]: 875 (sh) (110), 730 (130), 563 (sh) (290), 521 (420), 487 (510), 375 (sh) (1880), 285 (sh) (15 470), 259 (25 170). Conductivity (MeCN, 10^{-3} M solution at 298 K): Λ_M = 293 mho cm^2 mol^{-1}.

$[Mn^{III}_2(\mu\text{-}O)(\mu\text{-}OAc)_2(MeL)_2][ClO_4]_2\cdot H_2O$ (2b). Method A. This was synthesized by following a similar procedure as described for **2a**, however, using $NaClO_4\cdot H_2O$ instead of NH_4PF_6.

Method B. To a stirred mixture of $Mn(OAc)_3\cdot 2H_2O$ (0.200 g, 0.746 mmol), NaOAc (0.61 g, 0.746 mmol), and $NaClO_4\cdot H_2O$ (0.210 g, 2 mmol) in CH_3OH was added a solution of MeL (0.169 g, 0.746 mmol) in 5 mL of CH_3OH, and then four drops of glacial acetic acid were added to prevent the formation of **1a**. After 15 min of stirring a purplish brown precipitate started appearing. The solid was collected by filtration and washed thoroughly with CH_3OH and finally dried in vacuo. The solid thus obtained was dissolved in a minimum amount of MeCN, and 4−6 drops of glacial acetic acid was added. Then an equal volume of ethyl acetate was added and the solution allowed to stand at 273 K for 1−2 days. A crystalline purplish brown product was collected by filtration and dried in vacuo. Yield: 0.23 g, 67%.

Method C. To a stirred mixture of $Mn(OAc)_3\cdot 2H_2O$ (0.37 g, 1.38 mmol) and MeL (0.313 g, 1.38 mmol) in 8 mL of CH_3OH was added dropwise a solution of $HClO_4$ (0.12 mL of 70% $HClO_4$ dissolved in 2 mL of CH_3OH). Stirring the mixture for 5 min resulted in the formation of a purplish brown precipitate. The solid was collected by filtration, washed thoroughly with CH_3OH, and finally dried in vacuo. Recrystallization was achieved following the methodology as described in method B.Yield: 0.31 g, 50%.

All the three methods gave rise to identical products. Representative microanalytical data are presented here. Anal. Calcd for $C_{32}H_{42}N_6O_{14}Cl_2Mn_2$: C, 41.97; H, 4.60; N, 9.18. Found: C, 41.67; H, 4.80; N, 9.28. IR (KBr, cm^{-1}, selected peaks): 3420 (m, ν(OH)), 1575 (m, ν_{asym} (CO), 1440 (s, ν_{sym} (CO)), 1080 and 620 (s, $\nu(ClO_4^-)$, 770 (s, ν(MnOMn)). Absorption spectrum [in MeCN; λ_{max}, nm (ϵ, M^{-1} cm^{-1})]: 875 (sh) (110), 730 (130), 563 (sh) (290), 521 (420), 487 (510), 375 (sh) (1880), 285 (sh) (15 470), 259 (25 170). Conductivity (MeCN, 10^{-3} M solution at 298 K): Λ_M = 285 mho cm^2 mol^{-1}.

$[Mn^{IV}_2(\mu\text{-}O)_2(\mu\text{-}OAc)(MeL)_2][ClO_4]_3\cdot H_2O$ (3). The synthetic precedure described here is adapted from that of Pal et al.[12c]

The ligand MeL (0.5 g, 2.20 mmol) was dissolved in 15 mL of CH_3OH. To this was added solid $Mn(OAc)_3\cdot 2H_2O$ (0.59 g, 2.20 mmol). After the reaction mixture was stirred for 15 min at 298 K, it was filtered to reject an insoluble black residue (probably MnO_2). To the magnetically stirred filtrate 0.6 mL of 70% $HClO_4$ dissolved in 2 mL of CH_3OH was added dropwise at 273 K. After 45 min the greenish brown precipitate thus formed was collected by filtration, washed with CH_3OH (2−3 times) and then with CH_2Cl_2 to remove trace amounts of $[Mn^{III}Mn^{IV}(\mu\text{-}O)_2(\mu\text{-}OAc)(MeL)_2][ClO_4]_2\cdot H_2O$ (**1a**), and finally dried in vacuo. Yield: 0.29 g, 30%. Anal. Calcd for $C_{30}H_{39}N_6O_{17}Cl_3Mn_2$: C, 37.06; H, 4.00; N, 8.65. Found: C, 37.26; H, 4.07; N, 8.95. IR (KBr, cm^{-1}, selected peaks): 3420 (m, ν(OH)), 1570 (m, ν_{asym} (CO), 1438 (s, ν_{sym} (CO)), 1088 and 620 (s, $\nu(ClO_4^-)$, 766 (s, ν(MnOMn)). Absorption spectrum [in MeCN; λ_{max}, nm (ϵ, M^{-1} cm^{-1})]: 896 (sh) (35), 755 (90), 720 (sh) (65), 602 (355), 450 (sh) (1450), 300 (sh) (13 760), 253 (26 720). Conductivity (MeCN, 10^{-3} M solution at 298 K): Λ_M = 344 mho cm^2 mol^{-1}.

Reaction of $[Mn^{III}Mn^{IV}(\mu\text{-}O)_2(\mu\text{-}OAc)(MeL)_2][ClO_4]_2\cdot H_2O$ (1a) with Glacial Acetic Acid. To a green solution of **1a** (0.025 g, 0.029 mmol) in 5 mL of MeCN was added 1 mL of glacial acetic acid, and the solution was stirred for 20 h. The resulting purplish brown solution was reduced to ∼3 mL. To it an equal volume of ethyl acetate was added and allowed to stand for 36 h at 273 K. The purplish-brown precipitate thus formed was collected by filtration. The solid was identified as **2b**, based on its absorption spectrum in MeCN solution. Yield: 0.02 g (76%).

Reaction of $[Mn^{III}_2(\mu\text{-}O)(\mu\text{-}OAc)_2(MeL)_2][ClO_4]_2\cdot H_2O$ (2b) with Water. To a solution of **2b** (0.1 g, 0.11 mmol) in 10 mL of MeCN was added solid $NaClO_4\cdot H_2O$ (0.616 g, 4.384 mmol) and 2 mL of water. The resulting solution was stirred at 298 K for 3−4 h. The black precipitate (probably MnO_2) thus obtained was rejected by filtration, and the volume of the filtrate was reduced to ∼5 mL in vacuo and kept at 273 K for 12 h. The green crystalline precipitate thus obtained

was filtered out, thoroughly washed with water, and dried in vacuo. The solid was identified as **1a**, based on its absorption spectrum in MeCN solution. Yield: 0.015 g, 16%.

Reaction of $[Mn^{III}_2(\mu\text{-}O)(\mu\text{-}OAc)_2(MeL)_2][ClO_4]_2\cdot H_2O$ (2b) with Perchloric Acid. To a stirred suspension of **2b** (0.1 g, 0.11 mmol) in 4 mL of CH_3OH was added dropwise $HClO_4$ acid (0.075 mL of 70% $HClO_4$ dissolved in 1 mL of CH_3OH). Almost immediately a greenish brown precipitate started appearing. After 45 min it was filtered, the collected solid was washed first with CH_3OH and then with CH_2Cl_2 to remove trace amounts of **1a**, and the solid was dried in vacuo. Yield: 0.016 g, 15%. This solid was identified as **3**, based on its absorption spectral behavior.

Reaction of $[Mn^{III}Mn^{IV}(\mu\text{-}O)_2(\mu\text{-}OAc)(MeL)_2][ClO_4]_2\cdot H_2O$ (1a) with Perchloric Acid. To a stirred suspension of **1a** (0.08 g, 0.093 mmol) in 4 mL of CH_3OH was added $HClO_4$ (0.04 mL of 70% $HClO_4$ dissolved in 1 mL of CH_3OH). After 45 min, a greenish brown precipitate of **3** was collected by filtration, washed first with CH_3OH and then with CH_2Cl_2 (to remove trace amounts of **1a**), and dried in vacuo. Yield: 0.027 g, 30%.

Caution! *Perchlorate salts of compounds containing organic ligands are potentially explosive!*

Physical Measurements. Conductivity measurements were done with an Elico type CM-82T conductivity bridge (Hyderabad, India) with solute concentrations of ~1 mM. Spectroscopic measurements were made using the following instruments: IR (KBr, 4000−600 cm^{-1}), Perkin-Elmer M-1320; electronic, Perkin-Elmer Lambda 2; X-band EPR, Varian 109 C (fitted with a quartz dewar for measurements at liquid-dinitrogen temperature; the spectra were calibrated with diphenylpicrylhydrazyl, DPPH ($g = 2.0037$)).

X-ray Structure Determination of 1b. A greenish brown needle-shaped crystal of $[Mn^{III}Mn^{IV}(\mu\text{-}O)_2(\mu\text{-}OAc)(MeL)_2][BF_4]_2\cdot$MeCN (**1b**) (dimensions: 0.2 × 0.1 × 0.15 mm) was used for data collection at 293 K on an Enraf-Nonius CAD4-Mach diffractometer using graphite-monochromated Mo Kα radiation ($\lambda = 0.710\ 73$ Å). Lattice parameters were obtained from least-squares analyses of 25 machine-centered reflections. The experimental details are already reported in the literature.[27] Data were corrected for Lorentz and polarization effects; analytical absorption corrections were applied. The XTAL3.2 package[28] was used in absorption and all subsequent calculations, utilizing a PC-486 computer under MS-DOS version 5. The linear asbsorption coefficients, neutral atom scattering factors for the atom, and anomalous dispersion corrections for non-hydrogen atoms were taken from ref 29. The structure was solved by direct methods followed by subsequent difference Fourier syntheses. The function minimized during refinement by full-matrix least-squares methods was $\sum w(F_o - F_c)^2$, where $w = 1/\sigma(F)$. Anisotropic thermal parameters were used for only Mn, O, N (except the N atoms of two MeCN molecules), and C (except for the carbon atoms of the ligand coordinated to Mn(2) and those of the MeCN molecules which were refined isotropically). Hydrogen atom positions were calculated by assuming ideal geometries of the atoms concerned and their thermal parameters were not refined. Two boron atoms of disordered BF_4^- anions were not refined; however, the fluorine atoms were refined isotropically. For both of them, the apical fluorine atoms were unique, but the remaining three fluorines were disordered over three positions, with occupancies of 0.5, 0.25, and 0.25. All the C−N and C−C (N(4)−C(30)) bonds of one of the terminal MeL ligands (coordinated to Mn(2)) were restrained to have reasonable bond distances and angles. With the model used the structure converged moderately satisfactorily. Four reflections (*hkl*: 1,−1,1; 1,0,−1; 2,0,0; 2,2,1) were omitted in the final stages of refinement, as the peak profiles were extremely broad. These erroneous reflections were probably caused by the quality of crystal chosen for data collection. In fact, the quality of crystals obtained was not good. Crystal data and a summary of experimental results are collected in Table 1. Selected bond lengths and angles are listed in Table 2. Full details may be found in the Supporting Information. The refinement did not yield satisfactory *R* values; however, the refined model is sufficiently accurate for the description of the core structure of the complex. The relatively high *R* values are likely caused by (i) poor crystal quality which has caused weak scattering (>10 crystals were examined), (ii) the disorder associated with the MeL ligand coordinated to Mn(2) in the cationic part and also disorder in the tetrafluoroborate anions, and (iii) the large thermal motion of the solvent molecules.

Table 1. Crystal Data for $[Mn^{III}Mn^{IV}(\mu\text{-}O)_2(\mu\text{-}OAc)(MeL)_2][BF_4]_2\cdot$2MeCN (**1b**)

empirical formula	$C_{34}H_{43}N_8B_2F_8O_4Mn_2$
fw	910.6
temp, °C	20
radiation (λ, Å)	Mo Kα (0.710 73)
cryst syst	triclinic
space group	$P\bar{1}$
a, Å	10.283(2)
b, Å	13.874(5)
c, Å	16.152(5)
α, deg	65.74(3)
β, deg	84.24(2)
γ, deg	78.06(2)
V, Å^3	2055.094(1.169)
Z	2
F(000), electrons	934
ρ(calcd), g cm^{-3}	1.34
μ(Mo Kα), mm^{-1}	0.69
min/max transm coeff	0.9066/0.9068
no. of unique reflcns	7220
no. of reflcns used ($I > 3\sigma(I)$)	3738
no. of variables	413
R^a	0.112
$R_w{}^b$	0.119
goodness of fit	3.364

^{a} $R = \sum(F_o - F_c)/\sum F_o$. ^{b} $R_w = [\sum w(F_o - F_c)^2/\sum wF_o{}^2]^{1/2}$, $w = 1/\sigma(F)$.

Table 2. Selected Bond Lengths (Å) and Angles (deg) in the Cationic Part of $[Mn^{III}Mn^{IV}(\mu\text{-}O)_2(\mu\text{-}OAc)(MeL)_2][BF_4]_2\cdot$2MeCN (**1b**)

Mn(1)−O(1)	1.778(9)	Mn(2)−O(1)	1.82(1)
Mn(1)−O(2)	1.77(1)	Mn(2)−O(2)	1.813(9)
Mn(1)−O(3)	1.934(9)	Mn(2)−O(4)	2.18(1)
Mn(1)−N(1)	1.99(1)	Mn(2)−N(4)	2.23(1)
Mn(1)−N(2)	2.14(1)	Mn(2)−N(5)	2.12(1)
Mn(1)−N(3)	2.11(1)	Mn(2)−N(6)	2.10(2)
O(1)−Mn(1)−O(2)	86.4(5)	O(1)−Mn(2)−O(2)	83.9(4)
O(1)−Mn(1)−O(3)	93.7(4)	O(1)−Mn(2)−O(4)	89.2(4)
O(1)−Mn(1)−N(1)	95.1(4)	O(1)−Mn(2)−N(4)	93.4(5)
O(1)−Mn(1)−N(2)	174.5(5)	O(1)−Mn(2)−N(5)	92.2(5)
O(1)−Mn(1)−N(3)	92.3(5)	O(1)−Mn(2)−N(6)	177.0(5)
O(2)−Mn(1)−O(3)	94.4(4)	O(2)−Mn(2)−O(4)	88.6(4)
O(2)−Mn(1)−N(1)	89.6(5)	O(2)−Mn(2)−N(4)	97.9(4)
O(2)−Mn(1)−N(2)	90.2(5)	O(2)−Mn(2)−N(5)	175.7(6)
O(2)−Mn(1)−N(3)	177.9(4)	O(2)−Mn(2)−N(6)	93.5(5)
O(3)−Mn(1)−N(1)	170.5(5)	O(4)−Mn(2)−N(4)	173.2(5)
O(3)−Mn(1)−N(2)	90.9(4)	O(4)−Mn(2)−N(5)	89.5(5)
O(3)−Mn(1)−N(3)	87.3(5)	O(4)−Mn(2)−N(6)	89.2(5)
N(1)−Mn(1)−N(2)	80.5(5)	N(4)−Mn(2)−N(5)	84.1(5)
N(1)−Mn(1)−N(3)	88.9(5)	N(4)−Mn(2)−N(6)	88.5(5)
N(2)−Mn(1)−N(3)	91.0(5)	N(5)−Mn(2)−N(6)	90.3(6)
Mn(1)−O(1)−Mn(2)	93.5(4)	Mn(1)−O(2)−Mn(2)	93.9(4)

Magnetic Measurements. Solid-state magnetic data for **3** were collected in the range 25−300 K range with a locally built Faraday balance equipped with an electromagnet with constant gradient pole caps (Polytronic Corp., Bombay, India), Sartorius balance model 25-D/S (Göttingen, Germany), a closed cycle refrigerator, and a Lake Shore temperature controller (CTI Industries). All measurements were made at a fixed main field strength of ~10 kG. The details of the set up and experimental details are already reported in the literature.[27] The

(27) Ray, M.; Ghosh, D.; Shirin, Z.; Mukherjee, R. N. *Inorg. Chem.* **1997**, *36*, 3568.
(28) Hall, S. R., Flack, H. D., Stewart, J. M., Eds. *The XTAL 3.2 Reference Manual*; Universities of Western Australia, Geneva, and Maryland, 1992.
(29) *International Tables for X-ray Crystallography*; Kynoch Press: Birmingham, England, 1974; Vol. IV.

temperature dependence of the molar susceptibility was analyzed by using the van Vleck equation with the eigenvalues of the spin coupling Hamiltonian ($H = -2JS_1S_2$, $S_1 = S_2 = {}^3/_2$). This gives rise to eq 1,[30]

$$\chi = \frac{Ng^2\mu_B{}^2(2e^{2x} + 10e^{6x} + 28e^{12x})}{kT(1 + 3e^{2x} + 5e^{6x} + 7e^{12x})} \quad (1)$$

where χ is the molar susceptibility and $x = J/kT$. The fit of the data to the van Vleck equation was improved by the addition of a small amount of monomeric impurity and a temperature-independent paramagnetism (TIP) term. Thus eq 1 was modified in the following manner:

$$\chi = (1 - P)\chi' + P\chi_c + \text{TIP} \quad (2)$$

where χ is the total calculated susceptibility, χ' is the spin-coupled susceptibility calculated from eq 1, χ_c is the Curie law magnetic susceptibility for the monomeric Mn(II) impurity [$=Ng^2\mu_B{}^2S(S + 1)/3kT$], P is the fraction of the paramagnetic impurity, and TIP is the temperature-independent paramagnetism.

Solution-state magnetic susceptibility of **3** at 298 K was determined by the NMR technique of Evans[31] in MeCN with a PMX-60 JEOL (60 MHz) NMR spectrometer, and it was corrected for a diamagnetic contribution which was calculated to be -542×10^{-6} cm^3 mol^{-1} by using literature values.[30]

Electrochemical Measurements. Cyclic voltammetric experiments were performed by using a PAR model 370 electrochemistry system consisting of M-174A polarographic analyzer, M-175 universal programmer, and RE 0074 X-Y recorder. For coulometry an M-173 potentiostat/galvanostat, an M-179 digital coulometer, and an M-377A cell system were used. Potentials are reported at 298 K referenced to a saturated calomel electrode (SCE) and are uncorrected for the junction contribution. Details of the cell configuration are as described before.[32]

Results and Discussion

A. Synthesis and Properties of the Complexes. Triply bridged dimanganese complexes with $Mn^{III}Mn^{IV}$ (**1a**,**b**), Mn^{III}-Mn^{III} (**2a**,**b**), and $Mn^{IV}Mn^{IV}$ (**3**) oxidation levels have been isolated by a variety of disproportionation reactions using a common tridentate facially capping ligand, MeL. The synthetic aspect of binuclear Mn dimers with a common terminal coordination has a special relevance to its model (redox and core interconversion studies) behavior. The mixed-valence complex **1b** having BF_4^- as the counterion was prepared only to grow single crystals suitable for structural work, and the bulk material was characterized by absorption spectroscopy. Complex **2b** was synthesized to have a common ClO_4^- counterion for all the three Mn dimers $Mn^{III}Mn^{IV}$ (**1a**), $Mn^{III}Mn^{III}$ (**2b**), and $Mn^{IV}Mn^{IV}$ (**3**). All the complexes exhibit IR absorption peaks at ~1450 and ~1585 cm^{-1}, assigned to bridging acetate groups. A broad peak centered at ~3600 cm^{-1} is observed for all the complexes, excepting **1b**, consistent with the presence of water as solvent of crystallization. Characteristic IR absorptions for the Mn−O−Mn and Mn_2O_2 units are clearly observable. The characteristic ionic perchlorate (for **1a**, **2b**, and **3**) or hexafluorophosphate (for **2a**) absorptions were clearly observed in their IR spectra. The IR spectra of **1a** and **3** are almost superimposable, suggestive of the presence of closely similar molecular structures for these two complexes. The positive ion mass spectra (FAB) of **1a**, **2a**, and **3** (Figure S1, Supporting Information) clearly authenticate the identity of these complexes. The following molecular ion species have been identified: $[Mn^{III}_2(\mu\text{-O})(\mu\text{-OAc})_2(MeL)_2]^{2+}$ ($m/z = 698$); $\{Mn^{III}_2(\mu\text{-O})(\mu\text{-OAc})_2(MeL)_2\}\{PF_6\}^+$ ($m/z = 843$); $[Mn^{III}Mn^{IV}(\mu\text{-O})_2(\mu\text{-OAc})(MeL)_2]^{2+}$ ($m/z = 655$); $\{Mn^{III}Mn^{IV}(\mu\text{-O})_2(\mu\text{-OAc})(MeL)_2\}\{ClO_4\}^+$ ($m/z = 754.5$); $\{Mn^{IV}_2(\mu\text{-O})_2(\mu\text{-OAc})(MeL)_2\}\{ClO_4\}^+$ ($m/z = 754.5$). It should be noted, however, that complex **3** dissociates under experimental conditions and hence only a low abundant molecular ion peak was observed. Solution electrical conductivity data in MeCN support the expected electrolytic nature[33] of these complexes. It is to be noted here that **2a**,**b** and **3** are extremely moisture sensitive. In fact, with its presence **2a**,**b** get converted to the $\{Mn^{III}Mn^{IV}(\mu\text{-O})_2(\mu\text{-OAc})\}^{2+}$ core within 1 week (vide infra) and **3** gets converted to the same core almost instantaneously.

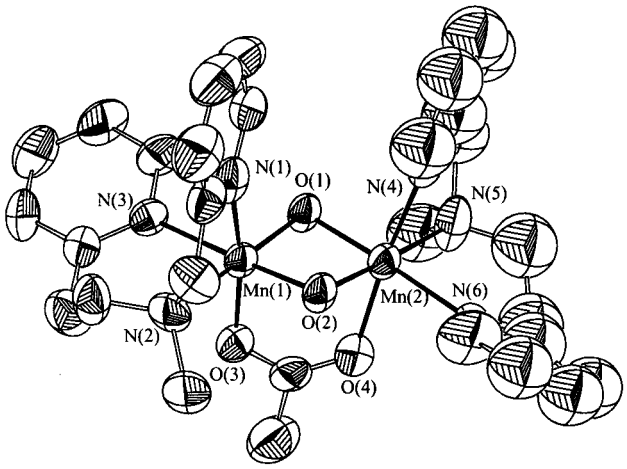

Figure 1. View of the $\{Mn^{III}Mn^{IV}(\mu\text{-O})_2(\mu\text{-OAc})(MeL)_2\}^{2+}$ cation in the crystals of the tetrafuoroborate salt **1b**. For clarity, hydrogen atoms are omitted and carbon atoms are not labeled.

B. Description of the Structure of $[Mn^{III}Mn^{IV}(\mu\text{-O})_2(\mu\text{-OAc})(MeL)_2][BF_4]_2\cdot 2MeCN$ (1b). The crystal structure of **1b** consists of a dimeric cation, two tetrafluoroborate anions, and two molecules of acetonitrile (Figure 1). Complex **1b** does not exhibit any crystallographically imposed symmetry, hence, resulting in the observation of distinct Mn^{III} and Mn^{IV} sites in the complex cation (vide infra). The tridentate ligand MeL binds each Mn atom in a facial configuration. The other three coordination sites are occupied by the two bridged oxo groups and the oxygen atom of a bridging acetate group. For each Mn center the coordination in the equatorial plane is provided by two oxide O atoms, an aliphatic N atom, and an ethylpyridine N atom. The two axial positions are coordinated by a methylpyridine N atom and an acetate O atom. As expected, the shortest bonds are the Mn−O bonds (Table 2).

Since Mn(III) is a d^4 Jahn−Teller sensitive ion, it is expected to show elongated axial Mn−N bonds, while the d^3 Mn(IV) center is expected to exhibit normal Mn−N bonds. This result has been revealed in the structures of all the Mn(III)/Mn(IV) dimers reported to date.[12a,17a] In the present complex the geometry around the Mn(2) center is axially elongated, and hence, it is expected to be the Mn^{III} ion.[34a] The $Mn-N_{ax}$ distance is appreciably longer (~0.1 Å than the $Mn-N_{eq}$ distances (Table 2). While the metal−ligand distances are within the normal range for Mn(1), it must be the Mn(IV) center.[32b] The $Mn-N_{ax}$ (methylpyridyl) distance is shorter than the $Mn-N_{eq}$ (ethylpyridyl) by 0.07 Å (Table 2). Thus the two Mn ions are structurally distinguishable (show different coordination environments around each of the Mn ions; vide infra), and hence, they have localized d-electrons. However, owing

(30) O'Connor, C. J. *Prog. Inorg. Chem.* **1982**, *29*, 203.
(31) Evans, D. F. *J. Chem. Soc.* **1959**, 2003.
(32) Ray, M.; Mukerjee, S.; Mukherjee, R. N. *J. Chem. Soc., Dalton Trans.* **1990**, 3635.
(33) Geary, W. J. *Coord. Chem. Rev.* **1971**, *7*, 81.

to inherent disorder of a MeL ligand which is coordinated to Mn(III), the accuracy of the crystal structure analysis of **1b** is not satisfactory enough for an unequivocal observation of delocalization of the valence of the manganese centers. The Mn···Mn distance (2.622(4) Å) is within the range (2.588(2)−2.741(1) Å) observed for other structurally characterized binuclear Mn complexes having a $\{Mn^{III}(\mu\text{-}O)_2Mn^{IV}\}^{3+}$ core with or without a supported acetate bridge.[12a] Bond angles suggest (Table 2) that the geometry around both the Mn centers is distorted octahedral. To each Mn center the aliphatic N atom is coordinated in the equatorial plane and the bond length is longer by 0.04/0.01 Å than the ethylpyridyl N atom.

There exist two very interesting features in this crystal structure. (i) The binding modes adopted by MeL for the Mn(III) and Mn(IV) centers are different. The aliphatic nitrogen atom (N(2)) is trans to one of the oxo bridges (O(1)) and cis to the other (O(2)) at the Mn(IV) center, whereas the corresponding aliphatic nitrogen (N(5)) is cis to O(1) and trans to O(2) at the Mn(III) center. This represents the second example of an asymmetric $\{Mn^{III}Mn^{IV}(\mu\text{-}O)_2(\mu\text{-}OAc)\}^{2+}$ core as a result of different binding modes adopted by a tridentate N-donor ligand at the Mn(III) versus the Mn(IV) site.[12a] (ii) Out of two pyridyl arms of MeL, the ethylpyridyl group is coordinated to each metal center only in the equatorial position. A similar observation was reported for a dioxodimanganese(III,IV) complex of a tetradentate pyridine-based ligand with chelate ring asymmetry (unsymmetrical ligation: a six- and a five-membered chelate ring).[15f] The present complex represents the first example of a dimanganese complex with a $\{Mn^{III}Mn^{IV}(\mu\text{-}O)_2(\mu\text{-}OAc)\}^{2+}$ core with a tridentate N-donor terminal ligand providing a similar chelate ring asymmetry.

C. Electronic Spectra. The electronic spectral behavior in MeCN solutions of $Mn^{III}Mn^{IV}$ (**1a**[11b] and **1b**), Mn^{III}_2 (**2a**,**b**), and Mn^{IV}_2 (**3**) complexes are the easiest means of their identification. The features are characteristic of all structurally characterized binuclear Mn complexes having similar electronic structures.[9b,f,g,14b,15c,g] The cases of **2a** and **3** are displayed in Figure 2.

D. Magnetism. The variable-temperature solid-state magnetic susceptibilities of $[Mn^{III}Mn^{IV}(\mu\text{-}O)_2(\mu\text{-}OAc)(MeL)_2][ClO_4]_2\cdot H_2O$ (**1a**), $[Mn^{III}_2(\mu\text{-}O)(\mu\text{-}OAc)_2(MeL)_2][PF_6]_2\cdot H_2O$ (**2a**), and $[Mn^{IV}_2(\mu\text{-}O)_2(\mu\text{-}OAc)(MeL)_2][ClO_4]_3\cdot H_2O$ (**3**) were measured using the Faraday method. For **1a** the measurements were performed in the temperature range 19.8−300 K, and for **2a** it was in the range 52−300 K. The magnetic behavior of **1a** is that expected for a pair of antiferromagnetically coupled Mn centers with a high-spin Mn^{III} ion ($S = 2$) and a Mn^{IV} ion ($S = {}^3/_2$) with $J = -144$ cm^{-1}.[11b] For **2a** only very weak ferromagnetic exchange coupling ($J = \sim+1$ cm^{-1}) was obtained.[11a]

Powdered samples of the Mn^{IV}_2 complex **3** were used for variable-temperature magnetic susceptibility measurements (25−300 K) (Figure 3). The μ_{eff}/Mn decreases gradually from a value of 2.30 μ_B at 300 K to 1.37 μ_B at 25 K. The fitting leads to a value of $J = -122.3$ cm^{-1} [$g = 2.00$ (fixed); $P = 0.1042$; TIP $= 1.1 \times 10^{-3}$ cm^3 mol^{-1}], which is in excellent agreement with those reported for related species[12a,c] and indicates intramolecular antiferromagnetic coupling. The solution-state magnetic moment of **3** was determined to be 2.40 μ_B, which is in good agreement with the solid-state value.

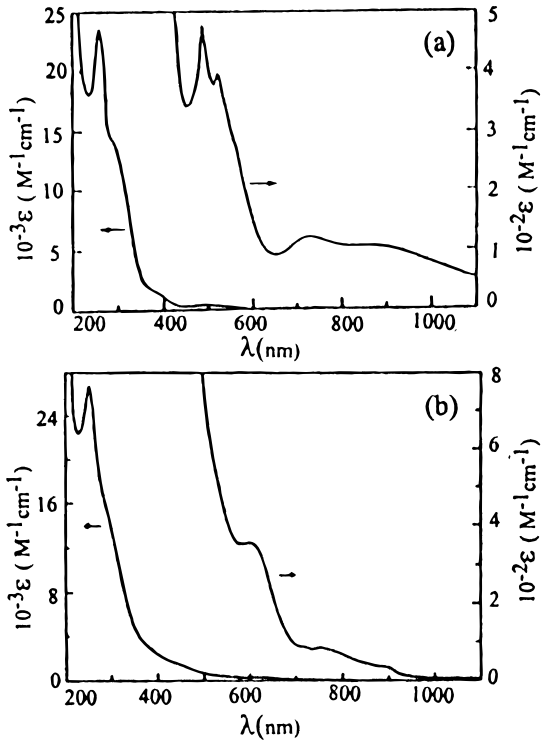

Figure 2. Electronic spectra of (a) $[Mn^{III}_2(\mu\text{-}O)(\mu\text{-}OAc)_2(MeL)_2][PF_6]_2\cdot H_2O$ (**2a**) and (b) $[Mn^{IV}_2(\mu\text{-}O)_2(\mu\text{-}OAc)(MeL)_2][ClO_4]_3\cdot H_2O$ (**3**) in MeCN.

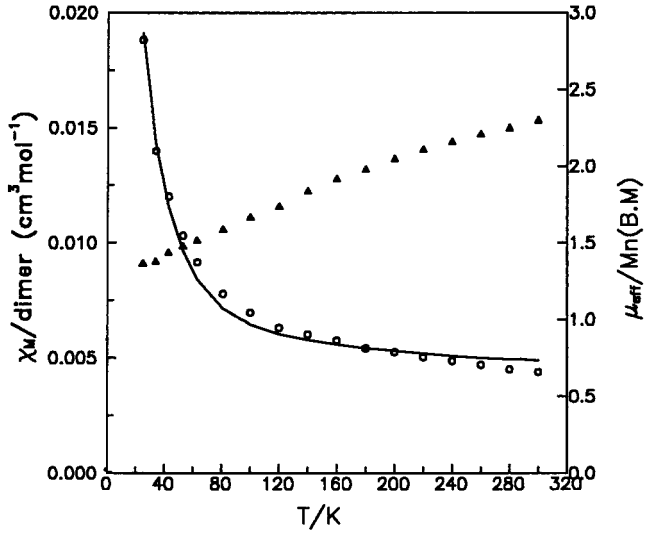

Figure 3. Plot of magnetic susceptibility (left scale) per dinuclear complex and effective magnetic moment (right scale) per metal (μ_{eff}/Mn) versus temperature for a polycrystalline sample of complex **3**. The solid line results from a least-squares fit of the susceptibility data to eq 2. See the text for fitting parameters.

E. EPR Spectra. The EPR spectrum of **1a** in dichloromethane at 77 K exhibits a characteristic 16-line ^{55}Mn hyperfine pattern centered near $g \sim 2.0$, representative of binuclear $Mn^{III}Mn^{IV}$ systems including the S_2 state of the Mn center of PS II.[11b] The Mn^{III}_2 complexes **2a**,**b** do not display any EPR signal, under our experimental conditions. Since

(34) (a) Although we succeeded in growing single crystals of Mn^{III}_2 complex **2b** from MeCN−ethyl acetate layering at 273 K, the X-ray data collected at 295 K using such a crystal (orthorhombic space group $Pca2_1$) has not allowed us to solve the structure satisfactorily, due to a poor data set and severe disorder associated with the terminal MeL ligands. However, the presence of the $\{Mn^{III}_2(\mu\text{-}O)(\mu\text{-}OAc)_2(MeL)_2\}^{2+}$ core is clearly observable in the difference Fourier map. The asymmetric unit contains two such dimeric units, and one of the axial ligands for each Mn(III) center is provided by methylpyridyl moiety, as has been observed for **1b**. (b) Unfortunately, we have not succeeded so far in growing single crystals of Mn^{IV}_2 complex **3** suitable for X-ray structural analysis.

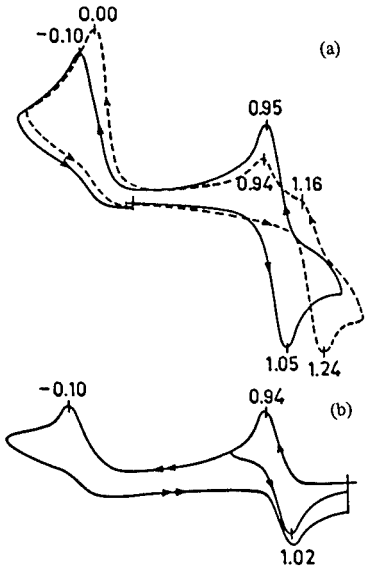

Figure 4. Cyclic voltammograms of (a) **1a** (—) and **2a** (- - -) and (b) **3** in MeCN (O.1 M TBAP) at a platinum electrode (scan rate 50 mV s^{-1}).

Mn^{IV}_2 complex **3** has an $S = 0$ ground state, it does not display prominent EPR signals at 77 K.

F. Redox Activity. Redox behaviors of Mn^{III}_2, $Mn^{III}Mn^{IV}$, or Mn^{IV}_2 complexes were investigated by CV in MeCN solution at a platinum working electrode, to have a better understanding of the properties of the core structures, upon redox manipulation. The cyclic voltammogram of **1a** shows (Figure 4) a quasireversible 1e$^-$ oxidation with $E_{1/2} = 1.0$ V to the Mn^{IV}_2 species as well as an irreversible 1e$^-$ reduction with $E_{pc} = -0.10$ V to the Mn^{III}_2 species.[11b] This behavior is common for all reported binuclear Mn complexes with $Mn^{III}(\mu\text{-O})_2Mn^{IV}$ or $Mn^{III}(\mu\text{-O})_2(\mu\text{-OAc})Mn^{IV}$ core structures. Complex **2a** exhibits a scan-rate dependent oxidative behavior.[11a] At a scan rate of 1000 mV s^{-1}, a reversible oxidative response with $E_{1/2} = 1.2$ V is observed. However, at moderate scan rates ($v = 20-500$ mV s^{-1}) it exhibits an anodic wave at 1.24 V and on scan reversal it exhibits two reductive waves at 1.16 V and at 0.94 V. On cycling of the scans between the potential limits 0.4 and 1.4 V, at the expense of the higher potential response the lower potential response grows.[11a] Complex **2a** also displays a reductive response in the negative side of SCE with $E_{pc} = 0.00$ V due to its reduction to supposedly $Mn^{III}Mn^{II}$ species. Its redox behavior at a scan rate of 50 mV s^{-1} is displayed in Figure 4. When coulometric oxidation was performed on **2a**, this Mn^{III}_2 complex transforms to the 1e$^-$ oxidized form of **1a**, i.e., the Mn^{IV}_2 species, due to an ECE mechanism.[11a] This means that a net 2e$^-$ oxidation occurs. This core transformation clearly demonstrates the facility of the ligand redistribution and metal redox reactions accompanied by protonation/deprotonation at the oxo bridge.

In the present investigation we have studied the cyclic voltammetric behavior of an isolated sample of **3**. It displays two 1e$^-$ reductive responses (Figure 4), one at $E_{1/2} = 0.98$ V which is reversible and an irreversible one at $E_{pc} = -0.10$ V. This behavior is identical, within experimental error, to that observed for complex **1a**. A clean well-formed cyclic voltammogram presented in Figure 4 documents the purity and authenticity of this Mn^{IV}_2 species. It is worth noting here that, in MeCN solution, **3** is stable only in very dry conditions. As for example, its color changes from brown to green ($Mn^{III}Mn^{IV}$ species) within 1 week. The identification of the product is done by its absorption spectral feature and CV. To bring about this transformation for **3**, a possibility to oxidize water exists.[35,36]

G. Nature of Synthetic Reactions. The isolation of the $[Mn^{III}Mn^{IV}(\mu\text{-O})_2(\mu\text{-OAc})(MeL)_2]^{2+}$ core in a reasonable yield (∼37−42%) from a MeCN reaction mixture containing "$Mn(OAc)_3\cdot 2H_2O$" as the starting material indicates that a disproportionation reaction occurred (eq 3):[14a,37]

$$3Mn^{III} \rightarrow Mn^{III}Mn^{IV} + Mn^{II} \quad (3)$$

Only three reports are known in the literature on the synthesis of a $[Mn^{III}Mn^{IV}(\mu\text{-O})_2(\mu\text{-OAc})]^{2+}$ core using "$Mn(OAc)_3\cdot 2H_2O$" as the starting material.[12d,13,14a]

Prior reports of the synthesis of the $\{Mn^{III}_2(\mu\text{-O})(\mu\text{-OAc})_2\}^{2+}$ core using "$Mn(OAc)_3\cdot 2H_2O$" as the starting material are also few.[8b,9a−c,f] The high-yielding (∼60−75%) synthesis of **2a** has been achieved following glacial acetic acid dependent disproportionation reaction of the initially formed mixed-valence complex, **1a**.[11a] The first step in this process involves protonation of the bridging oxo group. This protonation makes the III,IV complex a much stronger oxidant, permitting it to oxidize an unprotonated III,IV species to the IV,IV level while the protonated species would be initially reduced to the III,III level. Under the reaction conditions the stability of $[Mn^{III}_2(\mu\text{-O})(\mu\text{-OAc})_2(MeL)_2]^{2+}$ is significantly higher than that of $[Mn^{IV}_2(\mu\text{-O})_2(\mu\text{-OAc})(MeL)_2]^{3+}$ and hence the isolated species is **2a**.

The synthesis of $[Mn^{IV}_2(\mu\text{-O})_2(\mu\text{-OAc})(MeL)_2][ClO_4]_3\cdot H_2O$ **3** from the reaction mixture containing "$Mn(OAc)_3\cdot 2H_2O$", MeL, and $HClO_4$ in MeOH is also a case for disproportionation reaction as given in eqs 4[14c,37] and 5.[12a−c,37] It is worth noting

$$2[Mn^{III}_2(\mu\text{-O})(\mu\text{-OAc})_2(MeL)_2]^{2+} + 3H^+ \rightarrow [Mn^{IV}_2(\mu\text{-O})_2(\mu\text{-OAc})(MeL)_2]^{3+} + 2\text{“}[Mn^{II}(OH_2)]^{2+}\text{”} + 3HOAc + 2MeL \quad (4)$$

$$4[Mn^{III}Mn^{IV}(\mu\text{-O})_2(\mu\text{-OAc})(MeL)_2]^{2+} + 4H^+ \rightarrow 2\text{“}[Mn^{II}(H_2O)]^{2+}\text{”} + AcO^- + 2MeL + 3[Mn^{IV}_2(\mu\text{-O})_2(\mu\text{-OAc})(MeL)_2]^{3+} \quad (5)$$

here that the synthetic strategy involves initial formation of $[Mn^{III}_2(\mu\text{-O})(\mu\text{-OAc})_2(MeL)_2]^{2+}$ or $[Mn^{III}Mn^{IV}(\mu\text{-O})_2(\mu\text{-OAc})(MeL)_2]^{2+}$, which eventually leads to the isolation of **3**. The disproportionation of binuclear dimanganese(III,IV) complexes under acidic conditions is well documented.[12a−c,38]

The above two balanced equations provide a rationale for the behavior of **1** and **2** in the presence of $HClO_4$. In eq 4 50% and in eq 5 25% of the Mn ends up in the +2 oxidation state. This is in conformity with our observation that the yield of the dimanganese(IV) complex **3** is much reduced when dimanga-

(35) Thermodynamically, the Mn^{IV}_2 species $\{Mn^{IV}_2(\mu\text{-O})_2(\mu\text{-OAc})(MeL)_2\}^{3+}$ is capable of oxidizing water. The $E_{1/2}$ value of the $Mn^{IV}_2/Mn^{IV}Mn^{III}$ couple of **3** is ∼200 mV more positive than that of the O_2/H_2O couple (pH ∼ 7).[26b]

(36) However, we do not have any experimental proof of the proposal of O_2 production. Experiments to carefully look for (i) dioxygen production (!) and (ii) quantitative yield of the $Mn^{IV}Mn^{III}$ complex, for any possible ligand oxidation or degradation, are being planned.

(37) The light colored filtrate of our reaction mixture exhibits the characteristic six-line EPR spectrum of manganese(II). Hence the unisolated manganese remains in the +2 oxidation level.

(38) (a) Philouze, C.; Blondin, G.; Girerd, J.-J.; Guilhem, J.; Pascard, C.; Lexa, D. *J. Am. Chem. Soc.* **1994**, *116*, 8557. (b) Sarneski, J. E.; Brzezinski, L. J.; Anderson, B.; Didiuk, M.; Manchanda, R.; Crabtree, R. H.; Brudvig, G. W.; Schulte, G. K. *Inorg. Chem.* **1993**, *32*, 3265. (c) Sarneski, J. E.; Thorp, H. H.; Brudvig, G. W.; Crabtree, R. H.; Schulte, G. K. *J. Am. Chem. Soc.* **1990**, *112*, 7255.

Scheme 1

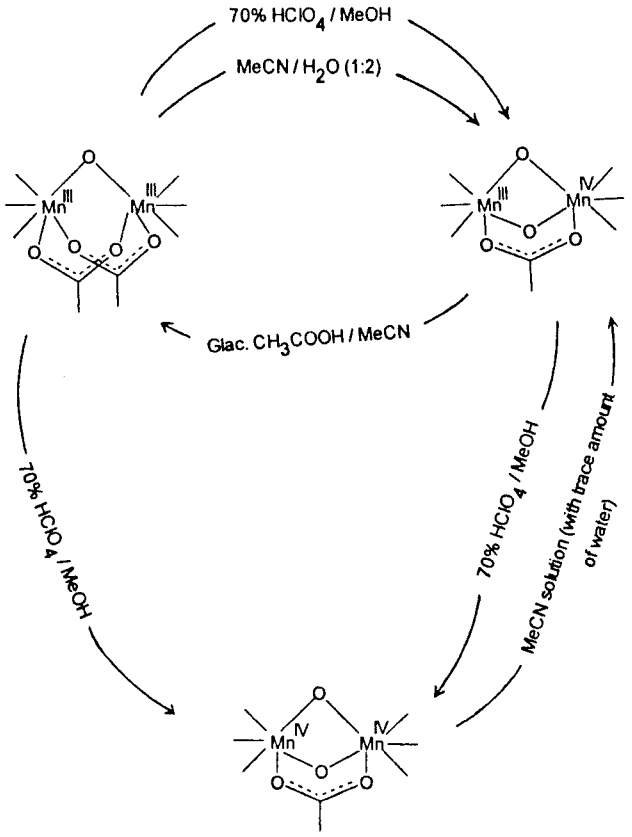

nese(III) complex **2b** was used as the starting material. This behavior could be due to the fact that **1a** is significantly more stable than **2b** in acidic solution.

H. Core Interconversions. Exhaustive core interconversion studies have been carried out to explore substitutional flexibility of the dimeric units present in **1a**, **2b**, and **3**, given the widely varied reaction conditions. The results are summarized in Scheme 1.

a. Reaction of $[Mn^{III}Mn^{IV}(\mu\text{-}O)_2(\mu\text{-}OAc)(MeL)_2][ClO_4]_2\cdot H_2O$ (1a) with Glacial Acetic Acid. The synthesis of **2b** from **1a** is a definitive case of an acid-catalyzed disproportionation reaction (vide supra).[11a]

b. Reaction of $[Mn^{III}Mn^{IV}(\mu\text{-}O)_2(\mu\text{-}OAc)(MeL)_2][ClO_4]_2\cdot H_2O$ (1a) with Perchloric Acid. The synthesis of the Mn^{IV}_2 complex **3** from **1a** by treatment with $HClO_4$ is most likely the consequence of a disproportionation reaction (vide supra). An equation that provides rationale for this reaction is already given in eq 5.

c. Reaction of $[Mn^{III}_2(\mu\text{-}O)(\mu\text{-}OAc)_2(MeL)_2][ClO_4]_2\cdot H_2O$ (2b) with Water. The synthesis of **1a** from the reaction between a MeCN solution of **2b** and water can be rationalized as follows. It is to be noted here that the yield is very poor, though. We propose the equilibrium in MeCN−H_2O medium, eq 6, to exist. The protonated species that is formed would be

$$[Mn^{III}_2(\mu\text{-}O)(\mu\text{-}OAc)_2(MeL)_2]^{2+} + H^+ \rightleftharpoons [Mn^{III}_2(\mu\text{-}OH)(\mu\text{-}OAc)_2(MeL)_2]^{3+} \quad (6)$$

$$[Mn^{III}_2(\mu\text{-}OH)(\mu\text{-}OAc)_2(MeL)_2]^{3+} + [Mn^{III}_2(\mu\text{-}O)(\mu\text{-}OAc)_2(MeL)_2]^{2+} \rightarrow [Mn^{III}Mn^{II}(\mu\text{-}OH)(\mu\text{-}OAc)_2(MeL)_2]^{2+} + [Mn^{III}Mn^{IV}(\mu\text{-}O)(\mu\text{-}OAc)_2(MeL)_2]^{3+} \quad (7)$$

$$[Mn^{III}Mn^{IV}(\mu\text{-}O)(\mu\text{-}OAc)_2(MeL)_2]^{3+} + H_2O \rightleftharpoons [Mn^{III}Mn^{IV}(\mu\text{-}O)_2(\mu\text{-}OAc)(MeL)_2]^{2+} + HOAc + H^+ \quad (8)$$

initially reduced to the III,II level $[Mn^{III}Mn^{II}(\mu\text{-}OH)(\mu\text{-}OAc)_2(MeL)_2]^{2+}$ (eq 7), which eventually decomposes to manganese(II) species.[37]

The reaction sequence is similar to that described for the reaction of **1a** with glacial acetic acid.[11a] It is worth mentioning here that aging of **2b** under moist conditions leads to the formation of **1a**, confirming the validity of eqs 6−8. Similar behavior under similar conditions has previously been reported by Christou et al.[10c] and Wieghardt et al.[9e,11e] with their Mn^{III}_2 dimeric systems.

d. Reaction of $[Mn^{III}_2(\mu\text{-}O)(\mu\text{-}OAc)_2(MeL)_2][ClO_4]_2\cdot H_2O$ (2b) with Perchloric Acid. The synthesis of the Mn^{IV}_2 complex **3** from **2b** by treatment with $HClO_4$ can be rationalized if we invoke that initially **2b** is transformed to **1b** via disproportionative oxidation of Mn(III) precursors. The initiation steps involved here are similar to that already described in eqs 6−8. Then it would probably involve protonation of the bridging oxo group. The protonated form of **1b** (hydroxo-bridged) may be a stronger oxidizing agent, permitting it to oxidize **1b** (oxo-bridged) to the species $[Mn^{IV}_2(\mu\text{-}O)_2(\mu\text{-}OAc)(MeL)_2]^{3+}$, while the protonated species would be initially reduced to the III,III level $[Mn^{III}_2(\mu\text{-}O)(\mu\text{-}OH)(\mu\text{-}OAc)(MeL)_2]^{2+}$ (eqs 9 and 10) which eventually decomposes to manganese(II) species.[37]

$$[Mn^{III}Mn^{IV}(\mu\text{-}O)_2(\mu\text{-}OAc)(MeL)_2]^{2+} + H^+ \rightleftharpoons [Mn^{III}Mn^{IV}(\mu\text{-}O)(\mu\text{-}OH)(\mu\text{-}OAc)(MeL)_2]^{3+} \quad (9)$$

$$[Mn^{III}Mn^{IV}(\mu\text{-}O)(\mu\text{-}OH)(\mu\text{-}OAc)(MeL)_2]^{3+} + [Mn^{III}Mn^{IV}(\mu\text{-}O)_2(\mu\text{-}OAc)(MeL)_2]^{2+} \rightarrow [Mn^{III}_2(\mu\text{-}O)(\mu\text{-}OH)(\mu\text{-}OAc)(MeL)_2]^{2+} + [Mn^{IV}_2(\mu\text{-}O)_2(\mu\text{-}OAc)(MeL)_2]^{3+} \quad (10)$$

I. Reactions of Dimanganese Cores with Chloride Ion. To shed light on the chloride ion−dependence of water oxidation, the reactivities of the dimanganese cores with chloride ion have been investigated by absorption spectroscopy and cyclic voltammetry.

When 2 equiv of $Et_4NCl\cdot xH_2O$ was added to the MeCN solutions of **1a**, **2b**, or **3**, the resulting solutions were always green. The absorption spectra of these solutions are characteristic of the presence of the $\{Mn^{III}(\mu\text{-}O)_2Mn^{IV}\}^{2+}$ core. It has been observed that **2b** reacts rather slowly (Figure S2, Supporting Information) whereas **1a** or **3** react almost instantaneously. The slower rate of reaction for **2b** is most probably due to its initial formation of **1a**, following the reaction sequence of eqs 6−8. The net effect is that reaction of $Et_4NCl\cdot xH_2O$ with **2b** or **3** brings about a redox process to generate **1a**.[39] In the case of **2b** it is an oxidation, and for **3** it is a reduction (vide infra).

When examined by CV, a MeCN solution of the Mn^{IV}_2 complex **3** and $Et_4NCl\cdot xH_2O$ (1:2 mole ratio) exhibits two oxidative responses, a broad anodic response at 1.06 V with its cathodic counterpart at 0.91 V and an additional response at $E_{1/2} = 0.73$ V (Figure 5). The anodic peak height (i_{pa}) of the response at 1.06 V is larger than the cathodic peak height (i_{pc}).

(39) Despite our sincere efforts, we have not been able to isolate any chloride(s)- ligated species in the solid state, from the reaction between **1a**, **2b**, or **3** and $Et_4NCl\cdot xH_2O$.

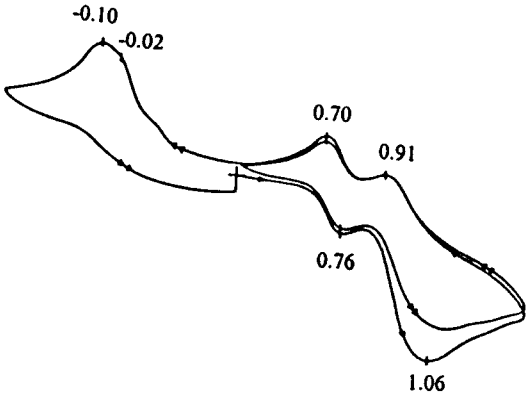

Figure 5. Cyclic voltammograms of a MeCN (0.1 M TBAP) solution of **3** and $Et_4NCl{\cdot}xH_2O$ (1:2 mole ratio) at a platinum electrode (scan rate 50 mV s^{-1}).

It is most probably due to simultaneous oxidation of chloride ion [$E°(Cl_2/Cl^-)$ is 1.36 V vs NHE][40] and the dimanganese core redox process (eq 11).

$$[Mn^{IV}{}_2(\mu\text{-O})_2(\mu\text{-OAc})(MeL)_2]^{3+} + e^- \rightleftharpoons [Mn^{IV}Mn^{III}(\mu\text{-O})_2(\mu\text{-OAc})(MeL)_2]^{2+} \quad (11)$$

The nature of this redox process, which is now oxidative, confirms our spectral results (vide supra). We propose that the $Mn^{IV}{}_2$ complex **3** reacts with Cl^- and water[36] to produce species such as $[Mn^{IV}Mn^{III}(\mu\text{-O})_2(OAc)(Cl)(MeL)_2]^+$ or $[Mn^{IV}Mn^{III}(\mu\text{-O})_2(Cl)_2(MeL)_2]^+$. The response at $E_{1/2} = 0.73$ V is due to either of the two suggested chloride-ligated species. Since the potential for the redox process of the Cl^--ligated Mn species is significantly lower (~200 mV) than that of the redox process eq 11, the Cl^--ligated species remains as $Mn^{IV}{}_2$ at potentials higher than ~0.8 V and then on scan reversal (cathodic scanning) gets reduced to the $Mn^{IV}Mn^{III}$ level. On scanning of the potential further down to −0.4 V, very interestingly two irreversible reductive responses were observed at −0.02 V and at −0.10 V, implying the presence of two closely related species. Recently, Pal et al. reported the chloride-ligated $Mn^{IV}{}_2$ complex having the core $\{Mn^{IV}{}_2(\mu\text{-O})_2(Cl)_2\}^{2+}$ using bpea as terminal ligand, and the redox behavior of our solution-generated chloride-ligated species is closely similar to that of the bpea system.[12a] Interestingly, in a MeCN solution containing 2 equiv of $Et_4NCl{\cdot}xH_2O$, the $Mn^{III}Mn^{IV}$ complex **1a** exhibits an identical behavior; however, this time the chloride-ligated response at $E_{1/2} = 0.73$ V is seen only during the second scan. This means that the Cl^- ion(s) gets coordinated only at the $Mn^{IV}{}_2$ level (Figure S3, Supporting Information).

The proposed reactivity of $Mn^{IV}{}_2$ complex **3** with water is supported by the following two controlled experiments. (i) When Cl_2 gas was bubbled through a MeCN solution of **1a**, no reaction occurred. (ii) When a trace amount of water was added to a MeCN solution of **3**, it immediately changes to **1a**.

From the above CV experiments we conclude that to suppress the increase in reduction potential for manganese that is observed upon successive oxidations, chloride(s) ions get coordinated to the manganese cluster.

J. Relevance to Biology. Synthetic procedures have been devised that allow convenient access routes to binuclear Mn complexes with variable oxidation levels and number of bridging oxo and acetato groups. As the first examples of the structural motifs $\{Mn^{III}{}_2(\mu\text{-O})(\mu\text{-OAc})_2\}^{2+}$, $\{Mn^{III}Mn^{IV}((\mu\text{-O})_2(\mu\text{-OAc})\}^{2+}$, and $\{Mn^{IV}{}_2(\mu\text{-O})_2(\mu\text{-OAc})\}^{3+}$ with a common asymmetric tridentate capping ligand, compounds **1**−**3** represent important models for the active site of OEC in PSII. First, this investigation convincingly demonstrates that, with the present complexes, it is possible to chemically or electrochemically generate or even isolate in the solid state dimanganese complexes at various oxidation levels, (III,IV), (III,III), and (IV,IV), without changing dramatically the overall structure of these dimers. However, the number of bridging oxo groups/acetate groups is one of the determining factors in achieving a desired oxidation state of manganese. Increasing the number of oxo groups from one to two and concomitantly decreasing the number of acetate groups from two to one stabilizes the manganese oxidation levels from (III,III) to (III,IV) or (IV,IV), depending on the reaction conditions. Second, the $\{Mn^{III}{}_2(\mu\text{-O})(\mu\text{-OAc})_2\}^{2+}$ core structurally mimics the Mn···Mn separation of 3.2 Å and the $\{Mn^{III}Mn^{IV}((\mu\text{-O})_2(\mu\text{-OAc})\}^{2+}$ and $\{Mn^{IV}{}_2(\mu\text{-O})_2(\mu\text{-OAc})\}^{3+}$ cores mimic the Mn···Mn separation of 2.7 Å of the Klein model.[6a] The $\{Mn^{III}Mn^{IV}(\mu\text{-O})_2(\mu\text{-OAc})\}^{2+}$ core has been structurally characterized. Third, they model the successive electron-transfer reactions from $Mn^{III}{}_2$ to $Mn^{III}Mn^{IV}$ to $Mn^{IV}{}_2$ oxidation levels, implicated to be operatrive during light-driven oxidation level change in the "*S*-states" eventually responsible for the oxidation of water. Since these redox reactions must be accomplished without the potential of the OEC becoming too high, the coupling of proton transfer to the electron transfer is of paramount importance, which is energetically favorable.[2b,5] Facile core interconversion ($Mn^{III}{}_2$ in **2a** to $Mn^{IV}{}_2$ in **3**) under oxidative conditions with concomitant protonation/deprotonation reactions at the bridging oxo groups in a readily accessible potential range strengthens the mechanistic proposals put forward for the function of OEC of PSII. Recently, site-directed mutagenesis studies have shown that several carboxylic acid and histidine residues are necessary for assembly and function of the Mn cluster in the PSII.[2b] This further strengthens the principal theme of this investigation.

Finally, on the basis of the present model studies, we propose that charge compensation during redox transitions in the water-oxidizing enzyme system is the functional role played by the uptake of Cl^-. These processes might provide the requisite adjustment in redox potential, the upper limit (~0.95 V vs NHE)[9f] of which is set by the potential of the primary chlorophyll photooxidant (P680). From our present model studies we strengthen the proposed roles of Cl^- put forward by Sheats et al.,[9f] with possible direct association with the Mn center of the active site.

Conclusion

Well-characterized examples of binuclear Mn complexes with all the three cores $\{Mn^{III}{}_2(\mu\text{-O})(\mu\text{-OAc})_2\}^{2+}$, $\{Mn^{III}Mn^{IV}((\mu\text{-O})_2(\mu\text{-OAc})\}^{2+}$, and $\{Mn^{IV}{}_2(\mu\text{-O})_2(\mu\text{-OAc})\}^{3+}$ have been prepared by a variety of disproportionation reactions, with the use of an asymmetric facially capping tridentate N-donor ligand. The mixed-valence core has been structurally characterized to reveal a novel asymmetric core structure. Systematic redox chemistry, core interconversion studies, and experiments aimed at understanding the reaction between Cl^- and **1a**, **2b**, and **3** were performed which shed substantial light on the possible role of Cl^- in the photosynthetic apparatus.

Acknowledgment. We gratefully acknowledge the financial assistance received from the Department of Science and Technology (DST) and the Council of Scientific and Industrial

(40) *CRC Handbook of Chemistry and Physics*, 64th ed.; CRC Press: Boca Raton, FL, 1983−1984; pp D-157.

Research (CSIR), Government of India. We also thank DST for the X-ray crystallographic facility in this department. We sincerely thank Sumitra Mukhopadhyay, Rajeev Gupta, and Debalina Ghosh for their technical assistance. Our special thanks are also due to Dr. Samiran Mahapatra for some of the key preliminary experiments.

Supporting Information Available: Listings of crystallographic experimental details, positional and isotropic thermal parameters, bond distances and angles, dihedral angles, anisotropic thermal parameters, least-squares planes, and hydrogen atom coordinates for compound **1b** (Tables S1−S8), magnetic data for **3** (Table S9), FAB-MS spectra of **1a**, **2a**, and **3** (Figure S1), electronic spectral monitoring of the course of reaction between $Et_4NCl·xH_2O$ and **2b** (Figure S2), and a cyclic voltammogram of **1a** with 2 equiv of $Et_4NCl·xH_2O$ (Figure S3) (29 pages). Ordering information is given on any current masthead page.

IC971514A